J Comput Aided Mol Des (2011) 25:583–597
DOI 10.1007/s10822-011-9443-z

Quantum mechanics study of the hydroxyethylamines–BACE-1 active site interaction energies

Carlos Gueto-Tettay · Juan Carlos Drosos · Ricardo Vivas-Reyes

Received: 29 November 2010 / Accepted: 7 June 2011 / Published online: 21 June 2011

Abstract The identification of BACE-1, a key enzyme in the production of Amyloid-β (Aβ) peptides, generated by the proteolytic processing of amyloid precursor protein, was a major advance in the field of Alzheimer's disease as this pathology is characterized by the presence of extracellular senile plaques, mainly comprised of Aβ peptides. Hydroxyethylamines have demonstrated a remarkable potential, like candidate drugs, for this disease using BACE-1 as target. Density Functional Theory calculations were employed to estimate interaction energies for the complexes formed between the hydroxyethylamine derivated inhibitors and 24 residues in the BACE-1 active site. The collected data offered not only a general but a particular quantitative description that gives a deep insight of the interactions in the active site, showing at the same time how ligand structural variations affect them. Polar interactions are the major energetic contributors for complex stabilization and those ones with charged aspartate residues are highlighted, as they contribute over 90% of the total attractive interaction energy. Ligand-ARG296 residue interaction reports the most repulsive value and decreasing of the magnitude of this repulsion can be a key feature for the design of novel and more potent BACE-1 inhibitors. Also it was explained why sultam derivated BACE-1 inhibitors are better ones than lactam based. Hydrophobic interactions concentrated at S1 zone and other relevant repulsions and attractions were also evaluated. The comparison of two different theory levels (X3LYP and M062X) allowed to confirm the relevance of the detected interactions as each theory level has its own strength to depict the forces involved, as is the case of M062X which is better describing the hydrophobic interactions. Those facts were also evaluated and confirmed by comparing the quantitative trend, of selected ligand-residue interactions, with MP2 theory level as reference standard method for electrostatic plus dispersion energies.

Keywords BACE-1 · Alzheimer's disease · Hydroxyethylamine inhibitors · DFT · X3LYP · Interaction energy · Counterpoise

C. Gueto-Tettay · J. C. Drosos · R. Vivas-Reyes (✉)
Grupo de Química Cuántica y Teórica, Programa de Química, Facultad de Ciencias Exactas y Naturales, Universidad de Cartagena, Cartagena, Colombia
e-mail: rvivasr@unicartagena.edu.co

C. Gueto-Tettay · J. C. Drosos
Grupo de Química Bioorgánica, Programa de Química, Facultad de Ciencias Exactas y Naturales, Universidad de Cartagena, Cartagena, Colombia

Introduction

Alzheimer's disease (AD) is a neurodegenerative disorder clinically characterized by progressive dementia that inevitably leads to incapacitation and finally to death [1]. The presence of amyloid plaques and congophilic angiopathy in the brain cortex and hippocampus has, for long, been recognized as a major pathological feature of AD [2]. These plaques primarily consist of a small 4 kDa Amyloid-β (Aβ) peptide, predominantly of 40 or 42 amino acids in length (Aβ40, Aβ42), and are generated by the proteolytic processing of a larger membrane bound precursor protein, known as the amyloid precursor protein (APP) [3]. Beta-site APP-cleaving enzyme-1 (BACE-1), an aspartyl protease also called β-Secretase or memapsin 2, is the first protease that processes APP in the pathway leading to the

production of Aβ and It has been considered for a long time as a therapeutic target for Alzheimer's disease in the development of inhibitor drugs for reduction of Aβ [4]. According to the enzyme characteristics, the transition state mimetic concept is the most widely used strategy for the design of BACE-1 inhibitors, an approach that has been used successfully to design inhibitors of other aspartyl proteases, most notably HIV protease [5].

Recently, it was described the first and second generation of novel hydroxyethylamines (HEAs) acting as BACE-1 inhibitors with; nanomolar potency in cells, favorable pharmacokinetic properties and orally bioavailables [6–11]. Despite significant progress in understanding the molecular and cellular effects of HEAs has been done [9, 12–14], a few theoretical studies, to the best of our knowledge, have been reported [15–18]. More particularly, such an approach is expected to shed some light onto the role of protein–ligand interactions for this system. The understanding of the interaction energies occurring in the active site is undoubtedly crucial to analyze how biological activity is affected with structural modifications of inhibitors and moreover, to determine which residues are essential in the active site according to their interaction energy contributions [19–22]. This approach is the basis of this study comprising the interaction energies of HEAs with each residue in the BACE-1 active site.

This work intends not only to aid in the rational design of new kind of BACE1 inhibitors but to explore in detail the interactions at enzyme active site, for this purpose we carried out a theoretical quantitative analysis of interaction energies for a representative set of HEAs–BACE-1 complexes at a quantum mechanics level, using M062X [23] and X3LYP [24] DFT functionals for comparative purpose, which significantly improve the accuracy for the estimation of some features like London dispersion forces [25], hydrogen-bonded and van der Waals complexes [24], respectively for each functional, key elements involved that must be considered during the description of the interaction phenomena.

The theoretical chemistry results obtained in this work are in agreement with the key interactions depicted, for HEAs/BACE-1 active site complexes, as part of the results of previous experimental findings [9, 26]. A remarkable case is the role of the charged aspartate residues, contributing over 40%, each one, to the total attractive interaction energy. This result, evaluated from a biological perspective, demonstrates that the presence of those residues is fundamental for the protein function and must be considered during the design of novel inhibitors as well as the positively charged ARG296 residue, which exhibits a repulsive ion–ion interaction that could be also modulated to improve complex stability.

Computational details

Structure collection

Preliminary the X-ray structures of 14 HEAs bound in the BACE-1 active site, reported by Demont et al. [6–11] were taken from the Brookhaven Protein Data Bank [27] under the following codes: 2VIE, 2VIY, 2VIZ, 2VJ6, 2VJ7, 2VJ9, 2VNM, 2VNN, 2WEZ, 2WF0, 2WF1, 2WF2, 2WF3 and 2WF4. Residues within a 5 Å radius from the center of 2VNM ligand were included for active site construction. This selection policy offered the same results independently of which ligand was used as sphere center (Fig. 1). The structure of each inhibitor and the 24 selected residues in the active site were isolated using Discovery Studio Visualizer [28] for further analysis. HEA inhibitor structures were modeled as protonated amines [6–12, 15, 16].

Geometry optimization

In order to obtain a better starting geometry, a short molecular dynamics simulation was carried out, considering only as flexible hydrogen atoms. For this purpose, MM3 force field was implemented in the Tinker package [29]. The system was allowed to stabilize at 315 K for 2 ps, the duration of the dynamic was 40 ps. The lowest energy conformation was used for subsequent steps. Then, the geometry of the protons was optimized at PM6 semiempirical level, using MOPAC 2009 [30], with the heavy atoms in the ligands and residues frozen. COSMO method was used to approximate the effect of the water surrounding the studied system [31]. Keywords MOZYME, MMOK, PM6-D, EPS = 78.4 and GNORM = 0.02 were used to activate: the Localized Molecular Orbital method [32], molecular mechanics correction to CONH bonds, PM6 Hamiltonian [33] with corrections for dispersion and hydrogen-bonding energies [34, 35], set the dielectric constant for the solvent and modifying energetic threshold to achieve the optimization criteria for high-precision work, respectively.

Determination of the protonation state

The issue of the protonation patterns of the key aspartyl groups in β-secretase has spurred widespread interest from both the experimental and theoretical perspectives. However, those studies, of the aspartate protonation states, have not yielded a consensus on which protonation condition (neutral diprotonated [36], di-deprotonated [37, 38] or monoprotonated [39–43] form) is preferred in the presence of inhibitor (Scheme 1).

In order to establish the preferred protonation state of catalytic aspartates at the HEAs/BACE-1 complexes, we

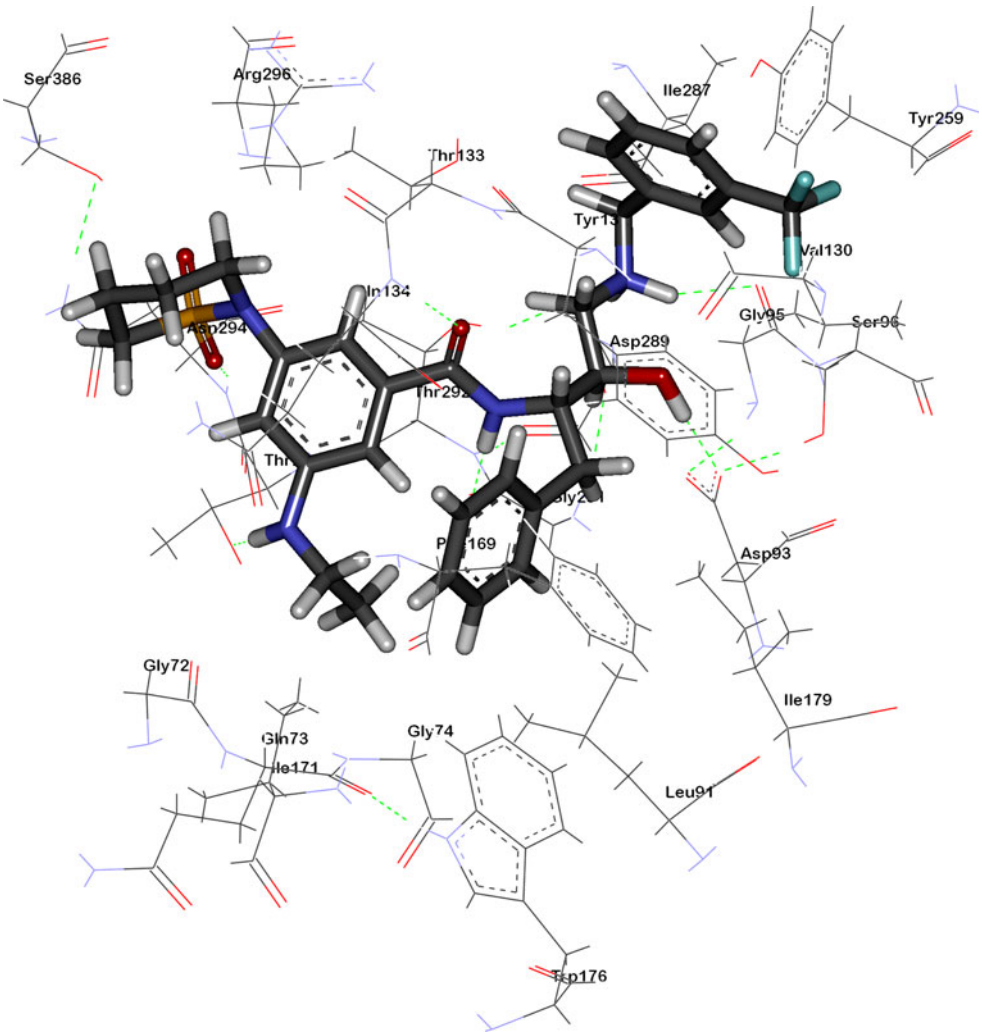

Fig. 1 Optimized structure of BACE-1 active site with 2VNM inhibitor, *green dashed lines* indicates the most relevant interaction contacts

used a similar approach as the previously one reported by Rajamani and Reynolds [41], which is based on the construction and subsequent computational chemistry calculation over a series of homodesmic reactions in order to compare energetically the most probable protonation states. The general reaction scheme (Scheme 2) represents the homodesmic system in which propionic acid is used as the reference state, considering its size and pK_a similarities to aspartic acid [44]. 2VNM/BACE-1 active site complex was used as the model structure for the analysis. The final geometry of the possible protonation states were obtained using the steps described above in section "Geometry optimization". Nevertheless, the relative energies, result of our calculations, were estimated using more recent theory levels which provide increased accuracy, namely M062X/6-31(d,p) and MOZYME PM6-DH2 methods using Gaussian09 [45] and MOPAC 2009 [30] program packages, respectively. In order to establish that no artifacts has been introduced during calculation, due to the only hydrogen atoms unlocked geometry optimization approach, an additional set of calculations was performed, but this time sidechains and hydrogen atoms were unlocked.

Data processing

Once determined the most probable BACE-1 active site aspartates protonation state in presence of HEA inhibitors, the separation of the active site cavity into individual fragments was necessary to isolate each residue energy contribution when interacting with each ligand.

Those cases where there are contiguous residues, protons were added to isolate each residue and a partial optimization, only to the newly added atoms, was performed using Gabedit as graphical interface [46] and semiempirical PM6 method as theory level (MOPAC 2009). Interaction energies (IE) were calculated from the single point energy differences between each ligand–residue complex and its constituent monomers, and expressed in kcal/mol. The counterpoise correction was considered and applied in order to correct for basis set superposition error (BSSE)

Scheme 1 Proton Locations considered for the monoprotonated, diprotonated and di-deprotonated Forms. [a]93i = proton present on the inner oxygen of the ASP93. [b]289o = proton present on the outer oxygen of the ASP289. [c]93o289i = proton present on the outer oxygen of ASP93 and inner oxygen of ASP289

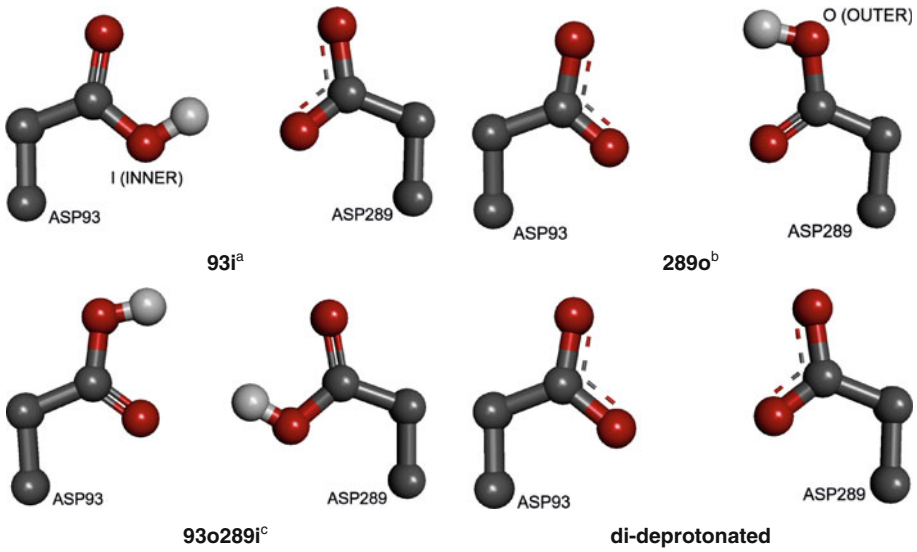

[a] 93i = proton present on the inner oxygen of the ASP93

[b] 289o = proton present on the outer oxygen of the ASP289

[c] 93o289i = proton present on the outer oxygen of ASP93 and inner oxygen of ASP289

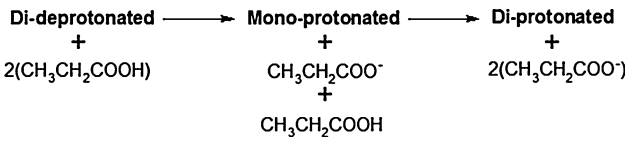

Scheme 2 Homodesmic reaction scheme used for comparison of protonation states

effect [47]. These calculations were performed using the Gaussian09 program package [45] with M062X [23] and X3LYP [24] DFT functionals and 6-311G (d,p) [48] as basis set.

In order to establish the accuracy of M062X and X3LYP DFT methods to estimate polar and hydrophobic interactions, MP2 interactions energy calculations (frozen core) were performed, for comparison, in those cases where couples do not follow the same pattern.

In the Table 1 are shown the structure of the HEA ligands as BACE-1 inhibitors. Geometry of optimized di-deprotonated BACE-1 active site/2VNM inhibitor complex and interaction and substitution zones in the 2VNM ligand is shown in Figs. 1 and 2, respectively.

Pearson's coefficient of variation

Pearson's coefficient of variation (CV) value is defined mathematically as the ratio of standard deviation to mean, and it is a rough measure of relative dispersion in probability distribution [49]. In this context, it is a measure of relative dispersion of the interaction energy values for each residue of the BACE-1 active site in the Hydroxyethylamine type inhibitors study group. This coefficient was calculated using the classical expression (1), where CV_i is the CV for i residue, N is the number of inhibitors in the study set, $\{X_{i1}, X_{i2}, \ldots, X_{iN}\}$, are the IE values for each inhibitor and i residue, and $\bar{X}_i$ the mean value for these observations.

$$CV_i = \frac{\sqrt{\frac{\sum_{j=1}^{N}\left(X_{ij}-\bar{X}_i\right)^2}{N}}}{\bar{X}_i} \times 100\% \quad (1)$$

Results and discussion

2VNM complex structure was used to carry out relative stabilities comparison of the three protonation states in presence of HEA inhibitors (Scheme 2), at semiempirical and DFT quantum mechanical calculation levels, using propionic acid as the reference state. A net charge of −2 was maintained for all three steps in the homodemisc reactions [41]. The results are given in Table 2. The computed relative energies indicate that the di-deprotonated aspartates form is clearly preferred over the diprotonated (charge = 0) and monopronated (charge = −1) forms with a difference in relative energy of ~354–359 and ~137–163 kcal/mol, respectively, according to the M062X/6-31G(d,p) DFT calculations. When a less restrained optimization was performed (considering the

Table 1 Base template structure, substituent structures and positions for the HEA inhibitors evaluated in this work

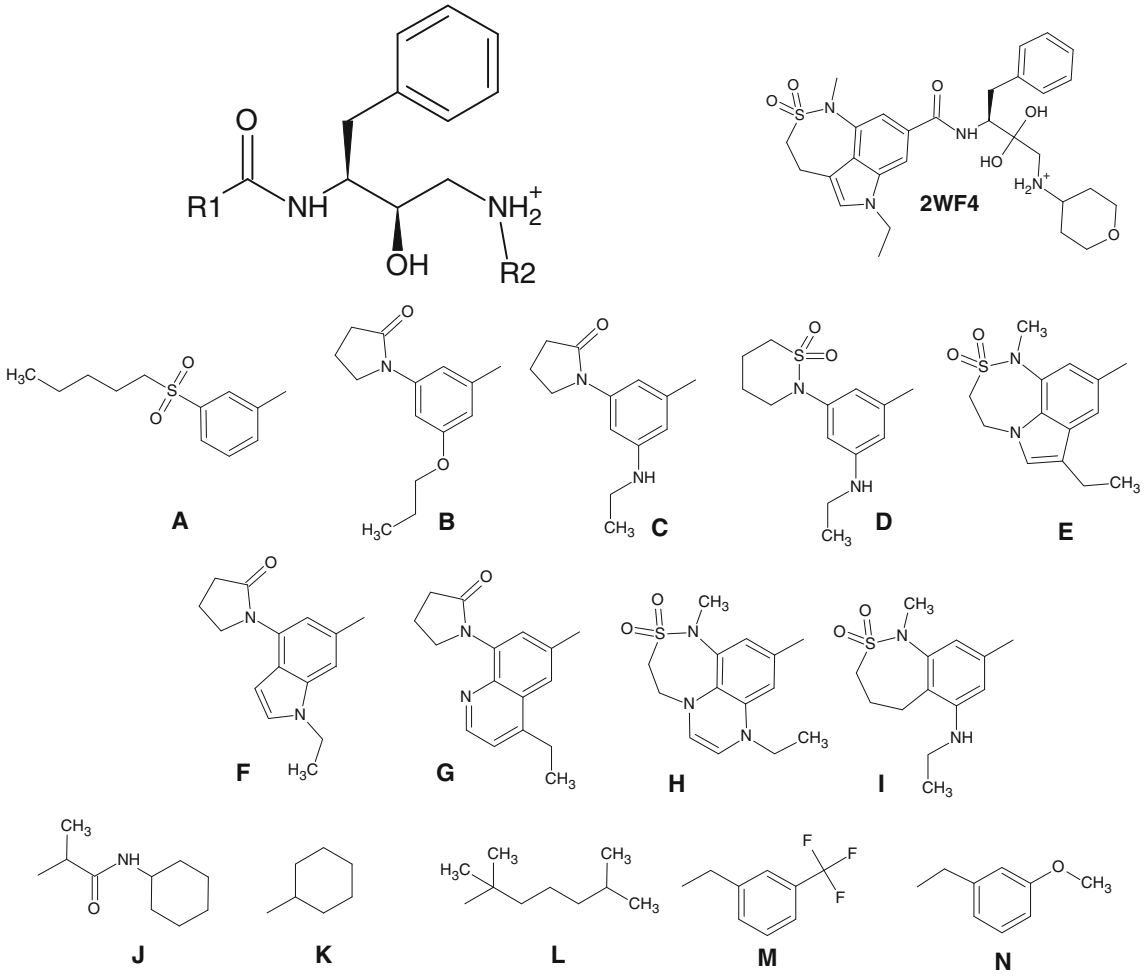

Ligand	R1	R2	Ligand	R1	R2
2VIY	A	J	2VNN	E	M
2VIZ	B	J	2WEZ	F	N
2VIE	C	L	2WF0	G	M
2VJ6	C	J	2WF1	E	N
2VJ7	C	M	2WF2	H	N
2VJ9	C	K	2WF3	I	N
2VNM	D	M			

sidechains and hydrogen atoms relaxation), lead to the same conclusion and discards any uncertainty on the energetic results (Table 2). Thus the calculations suggest that the di-deprotonated state (charge = −2) is preferred for BACE-1 in presence of HEA inhibitors. These results are in agreement with Hyland et al. finding, where the di-deprotonated has been reported to be favored in the presence of a reduced amide transition state isostere [37, 38]. Furthermore, MOZYME PM6-DH2 semiempirical calculations also lead to the same conclusions as can be seen in Fig. 3. Hydroxyl and protonated amine moieties on the ligands interact directly with ASP93 and ASP289 residues, respectively (Fig. 4). The forced rotation of hydroxyl moiety in carboxylic acid groups and/or ligands in presence of a proton in ASP93 and/or ASP289 residues leads to monoprotonated and diprotonated complexes destabilization; protonatation state configurations with a proton present on the outer oxygen of ASP289 residue (98o, 93i289o, 93o289o) tend to be the least favored due to improper torsions in hydroxyl group of this residue

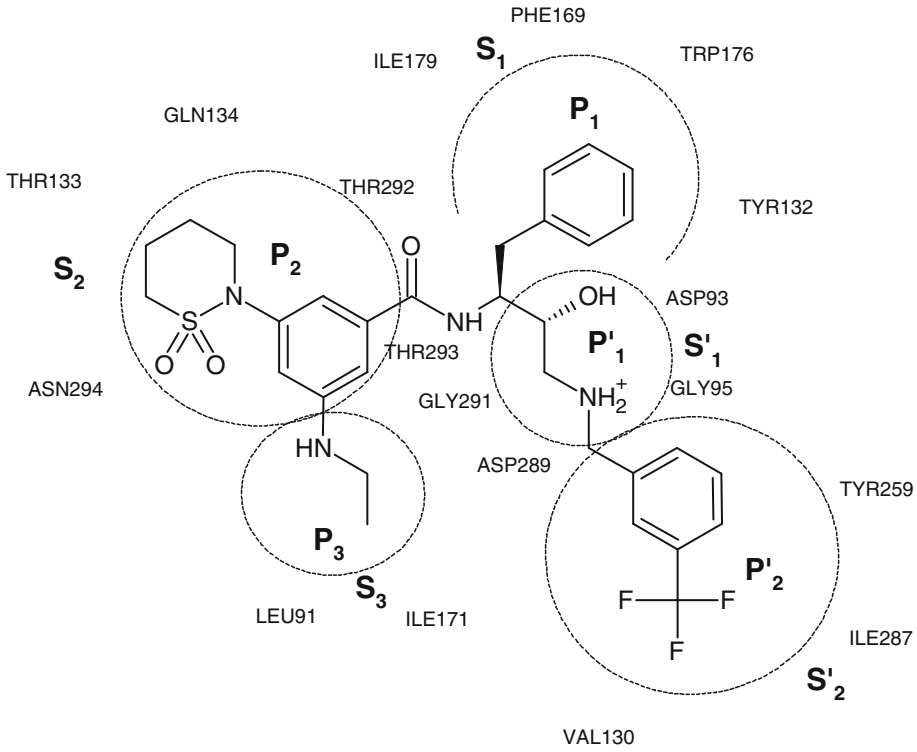

Fig. 2 BACE-1 active site subpockets and ligand interaction zones. 2VNM inhibitor is displayed in the background as reference

(Fig. 4b). Additionally, protonated ASP93 induce hydroxyl group rotation on the ligand respecting to di-deprotonated form (Fig. 4d), especially when the proton is present on the outer oxygen of ASP93 residue (Fig. 4c). In all cases, hydroxyl rotations are made in order to avoid steric clashes of interacting groups. Counterpoise interaction energy, only calculated for the minimum energy conformations for the individual states, between the ligand and the aspartate residues also support this idea (Table 2).

The counterpoise corrected electronic interaction energies between the active site residues and each ligand of the first and second generation of HEA inhibitors using M062X DFT functional is summarized on Table 3. The ligand-residues IE values show that polar interactions are the major energetic contributors for BACE-1-inhibitor complex stabilization. Tables 3 and 4 show the relative importance of the ASP93 and ASP289 charged polar residues as a portion of the active site. In each case, aspartate

Table 2 Relative energies (kcal/mol) for the di-deprotonated, monoprotonated and diprotonated states

Protonation state	H optimization[a]			SD + H optimization[b]	
	M062X	MOZYME PM6-DH2	IE[c]	M062X	MOZYME PM6-DH2
Monoprotonated					
289i	142.12	83.90		138.36	73.83
289o	162.87	95.61		154.59	79.51
93i	137.67	78.44	−109.82	133.27	71.31
93o	140.63	83.77		132.69	72.64
Diprotonated					
93i289i	354.01	182.64		351.10	160.29
93i289o	358.76	181.21		346.42	161.52
93o289i	336.22	177.97	−28.70	331.21	165.31
93o289o	357.33	185.72		342.87	158.26
Di-deprotonated	0.00	0.00	−213.80	0.00	0.00

[a] Only hydrogen atoms geometry optimization

[b] Sidechain and hydrogen atoms geometry optimization

[c] Interaction energy calculated between the 2VNM ligand and aspartates residues for each protonation state using M062X/6-31G(d,p)

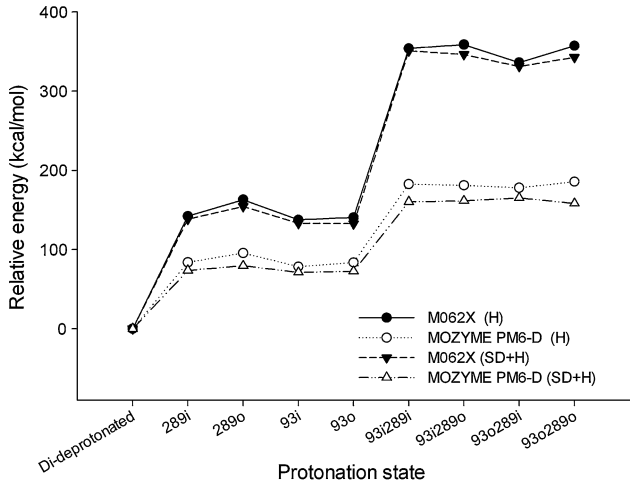

Fig. 3 Protonation state configurations relative energies calculated for M062X DFT and MOZYME PM6-D methods. Hydrogen (H) and sidechain plus hydrogen (SD + H) partial optimization results comparison

residue is responsible for 40–45% on average (Table 5) according to the sum of the average interaction energies. From a chemical point of view, when it is considered the charged nature of the aspartates (negative) and ligand (positive) species, the noticeable residue-ligand interaction energies are evident. This might happen as a consequence of the conjugated base-acid system formation and/or the favorable ion–ion interactions, both complementary electronic events.

Most of the polar residues contribute positively to the total interaction energy. Nevertheless, just ASN294, GLN134 and the triplet of threonine residues (133, 292, and 293) exhibit remarkable interaction energy values as they have a privileged place in the active site that leads to favorable polar contacts and/or sidechain-backbone hydrogen bonds formation with several fragments of the ligands. The same principle is applied to glycine residues (GLY95, GLY291) that despite of its small size has the capability to interact by its backbone.

On the other hand, hydrophobic interactions, mainly concentrated at S1 zone by LEU91, VAL130, PHE169, ILE171, TRP176 and ILE179 residues (Fig. 1), tend to be less favorable (in terms of IE) than polar ones, even repulsive in some cases. For most of these non-polar residues, discrete variations are found for the IE values (Table 5). This behavior is due to the fact that all ligands share a phenyl common moiety at P1 zone interacting directly with the mentioned monomers. In this no polar interactions set it is noticeable those formed with PHE169 amino acid, which is characterized by an aromatic π–π contact that decrease its IE value. The calculation of this kind of interactions is very sensitive to theory level and their description with more adequate functional provided better results. This influence is discussed elsewhere in this paper.

In contrast, ARG296 residue reports the most repulsive interaction on BACE-1 active site, being responsible for at least 90% of the total repulsive interactions. This unfavorable value is easily explained by taking into account that in biological conditions, both amino acid and ligand are always positively charged systems (this charged state

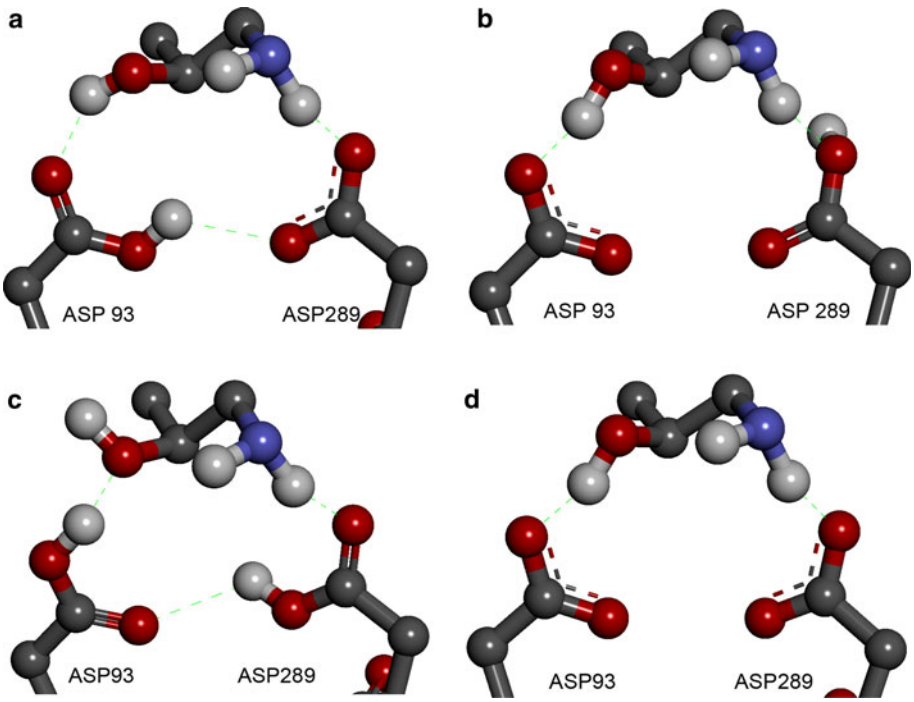

Fig. 4 Snapshots of aspartate residues in the active site of the monoprotonated; **a** (93i) and **b** (289o), diprotonated; **c** (93o289i) and di-deprotonated **d** forms

Table 3 Counterpoise corrected electronic interaction energies between amino acid residues at the BACE-1 active site and HEA ligands calculated from M062X DFT functional (energies are reported in kcal/mol units)

Lactams								Sultams						
M062X	2VIE	2VIZ	2VJ6	2VJ7	2VJ9	2WEZ	2WF0	2VIY	2VNM	2VNN	2WF1	2WF2	2WF3	2WF4
Polar residues														
ASN294	−3.66	−3.60	−1.88	−2.82	−2.51	−4.07	−3.52	−5.55	−7.64	−10.35	−8.86	−7.14	−8.76	−7.70
GLN134	−9.43	−9.12	−9.63	−8.85	−9.21	−12.18	−11.43	−9.16	−7.76	−9.33	−10.13	−11.14	−9.71	−12.73
GLN73	−1.34	−1.35	−1.44	−1.10	−2.45	−1.84	−1.64	−0.62	−1.09	−1.04	−1.37	−1.38	−0.69	−1.42
SER386	−2.57	−2.39	−2.41	−2.25	−2.43	−2.15	−1.95	−0.91	1.86	1.47	−2.08	1.00	1.05	1.33
SER96	2.99	3.74	3.97	3.01	−0.18	4.81	−1.47	−0.67	3.08	−2.11	−0.59	3.95	4.68	0.07
THR133	−7.03	−5.35	−5.49	−5.46	−5.45	−4.94	−4.61	−2.62	−4.56	−4.36	−4.67	−4.12	−5.63	−6.90
THR292	−8.35	−8.80	−3.99	−7.93	−4.71	−9.33	−4.73	−2.52	−7.86	−4.52	−6.54	−4.33	−8.96	−6.86
THR293	−9.76	−8.87	−11.87	−10.16	−11.37	−9.59	−9.05	−6.49	−10.87	−3.21	−2.48	−6.83	−8.88	−9.10
TYR132	−4.21	−5.51	−5.28	−3.56	−3.88	−6.41	−4.98	−5.19	−5.23	−4.75	−6.19	−6.48	−4.47	−2.31
TYR259	−2.22	−1.81	−1.79	−0.38	−1.90	−0.93	−1.58	0.93	−0.49	−0.23	−1.20	−1.69	−0.53	−2.99
Charged residues														
ARG296	35.52	32.86	32.39	35.50	36.15	32.58	34.17	20.11	23.80	23.33	25.95	24.61	22.71	25.22
ASP289	−107.26	−111.62	−110.06	−115.98	−109.92	−108.66	−110.77	−112.51	−113.96	−113.21	−104.16	−106.59	−108.21	−109.40
ASP93	−92.91	−102.16	−103.27	−98.47	−96.02	−101.78	−99.42	−105.00	−98.55	−97.63	−97.62	−93.70	−98.29	−106.59
Nonpolar residues														
GLY291	−3.23	−2.96	−1.85	−2.20	−2.13	−2.40	−2.92	−3.10	−2.63	−2.71	−2.87	−2.86	−3.32	−3.98
GLY72	−3.49	−1.00	−3.19	−3.21	−3.47	−3.91	−3.69	−1.84	−3.50	−3.68	−3.80	−3.82	−2.18	−5.14
GLY74	2.31	3.26	1.82	2.10	1.78	−0.62	1.48	1.84	−0.43	−0.09	−0.18	−0.24	2.08	1.87
GLY95	−5.82	−11.68	−11.80	−9.10	−7.09	−8.91	−9.41	−11.69	−8.31	−8.51	−8.51	−9.01	−9.31	−8.84
ILE171	0.13	0.12	0.11	0.27	−0.05	0.37	0.75	0.48	0.25	0.24	0.19	0.97	0.01	0.09
ILE179	−0.26	−0.60	−0.59	−0.04	−0.53	−0.49	−0.46	−0.56	−0.51	−0.44	−0.63	−0.45	−0.23	−0.47
ILE287	0.35	−0.42	−0.53	−0.60	−0.63	−0.46	−0.57	−0.40	−0.29	−0.43	−0.34	−0.08	−0.23	−0.19
LEU91	−1.35	−0.48	−1.69	1.60	−1.60	−1.60	−1.38	−1.64	−1.43	−1.74	−1.42	−1.46	−1.43	−1.83
PHE169	−3.60	−4.08	−3.29	−3.50	−3.46	−3.94	−4.05	−3.44	−3.73	−3.48	−3.26	−4.02	−3.36	−3.57
TRP176	−0.50	−0.84	−0.49	−0.43	−0.23	−0.41	−0.83	−0.50	−0.27	−0.38	−0.53	−0.23	−0.30	−0.24
VAL130	−0.33	0.64	0.85	−0.27	0.00	−0.16	−0.26	0.60	−0.23	−0.24	−0.20	−0.06	−0.17	−0.04

Table 4 Counterpoise corrected electronic interaction energies between amino acid residues at the BACE-1 active site and HEA ligands calculated from X3LYP DFT functional (energies are reported in kcal/mol units)

Lactams								Sultams						
X3LYP	2VIE	2VIZ	2VJ6	2VJ7	2VJ9	2WEZ	2WF0	2VIY	2VNM	2VNN	2WF1	2WF2	2WF3	2WF4
Polar residues														
ASN294	−0.96	−0.79	1.10	−0.27	0.24	−1.74	−1.13	−3.12	−3.58	−5.79	−4.32	−2.78	−4.92	−3.49
GLN134	−3.93	−1.69	−1.79	−1.81	−2.21	−3.75	−3.55	−1.71	−0.16	0.79	−1.60	−2.37	−1.91	−4.88
GLN73	−0.09	−0.23	−0.21	0.26	−1.05	−0.44	−0.36	−0.57	−0.10	−0.12	−0.07	−0.50	1.15	0.22
SER386	−2.11	−2.07	−2.04	−1.87	−2.05	−1.83	−1.67	−0.26	2.05	1.53	−1.84	1.13	1.14	1.40
SER96	4.43	6.19	6.55	4.51	0.35	7.11	0.05	1.52	4.90	−0.46	1.55	5.83	6.52	0.46
THR133	−3.07	−1.55	−1.58	−1.52	−1.45	−0.22	−0.71	0.98	−0.12	0.08	0.30	1.17	−1.09	−1.89
THR292	−3.17	−2.73	1.72	−2.45	1.46	−4.19	0.31	3.42	−2.40	0.75	−1.65	1.18	−3.97	−0.86
THR293	−5.30	−3.88	−7.46	−5.98	−6.81	−4.64	−3.39	−2.73	−7.06	0.75	1.74	−3.20	−4.32	−3.23
TYR132	3.89	3.84	3.53	6.19	2.35	2.04	3.94	3.63	4.16	4.40	1.34	1.85	3.61	4.19
TYR259	0.00	−0.11	−0.16	2.25	0.95	1.45	0.25	3.39	2.36	2.42	1.24	−0.19	1.64	−0.32
Charged residues														
ARG296	37.39	34.83	34.34	37.42	38.26	33.82	35.35	21.19	25.37	25.06	28.06	26.35	24.54	27.77
ASP289	−104.73	−108.81	−107.39	−113.64	−107.64	−106.36	−108.86	−109.76	−111.55	−110.89	−101.35	−104.46	−106.42	−106.18
ASP93	−90.88	−99.72	−100.36	−96.34	−93.32	−98.71	−96.95	−102.51	−95.84	−94.52	−94.91	−90.87	−96.27	−102.84
Nonpolar residues														
GLY291	0.14	1.34	1.69	1.04	1.48	1.26	0.46	−0.08	0.73	1.14	0.52	0.52	−0.05	0.56
GLY72	−2.84	−0.65	−2.35	−2.69	−2.68	−3.13	−3.01	−1.75	−2.91	−2.88	−2.90	−3.00	−0.93	−4.06
GLY74	3.71	5.60	2.99	3.30	2.99	0.20	2.25	1.81	0.27	0.34	0.43	0.13	2.37	2.35
GLY95	−2.25	−8.14	−8.27	−6.11	−4.55	−5.66	−6.47	−8.17	−5.40	−5.31	−5.02	−6.26	−6.25	−6.41
ILE171	0.84	0.72	0.93	0.77	1.15	1.13	1.40	0.78	0.95	1.18	1.02	1.45	1.18	1.01
ILE179	1.18	0.87	0.91	1.40	0.88	0.91	0.97	0.66	1.07	1.02	0.78	0.97	1.11	0.65
ILE287	1.30	0.12	−0.05	−0.26	0.97	−0.10	−0.24	0.10	−0.06	−0.11	−0.03	0.16	0.03	1.61
LEU91	0.95	2.60	0.60	2.89	0.69	0.61	0.55	0.03	1.02	0.30	0.36	0.60	0.45	0.20
PHE169	−1.13	−1.16	−0.82	−0.94	−1.29	−1.14	−0.95	−0.89	−1.07	−1.14	−0.80	−1.18	−0.90	−1.14
TRP176	1.28	0.69	1.03	0.88	1.18	1.11	0.83	0.75	1.11	1.00	0.85	1.20	0.88	1.03
VAL130	0.23	1.56	1.83	−0.02	−0.04	−0.07	−0.08	1.43	0.00	−0.02	−0.11	0.10	−0.06	−0.07

Table 5 Statistic analysis for the study set

M062X	ASN294	GLN134	GLN73	SER386	SER96	THR133	THR292	THR293	TYR132	TYR259
Polar residues										
Mean[a]	−5.58	−9.99	−1.34	−0.89	1.81	−5.09	−6.39	−8.47	−4.89	−1.20
Contribution[b] (%)	2.30	4.12	0.55	0.37	−0.74	2.10	2.63	3.49	2.02	0.50
CV[c]	−50.00%	−14.00%	−34.00%	−200.00%	137.00%	−22.00%	−35.00%	−33.00%	−24.00%	−83.00%
M062X			ARG296				ASP289			ASP93
Charged residues										
Media			28.92				−110.17			−99.39
Contribution (%)			−11.93				45.44			40.99
CV			20.00%				−3.00%			−4.00%
M062X	GLY291	GLY72	GLY74	GLY95	ILE171	ILE179	ILE287	LEU91	PHE169	TRP176	VAL130
Non-polar residues											
Media	−2.80	−3.28	1.21	−9.14	0.28	−0.45	−0.34	−1.25	−3.63	−0.44	0.01
Contribution (%)	1.15	1.35	−0.50	3.77	−0.12	0.18	0.14	0.51	1.50	0.18	0.00
CV	−20.00%	−31.00%	103.00%	−18.00%	101.00%	−37.00%	−74.00%	−71.00%	−8.00%	−45.00%	4,171.00%

[a] Average of the interaction energy for each residue in the study set. Mean values are expressed in kcal/mol units

[b] Contribution calculated based on the sum of average interaction energy

[c] Pearson's coefficient of variation

was considered for calculations), therefore a high repulsion is expected. This finding is consistent with recent structural modification on the ligand at P2 zone, used as a new approach to HEA design to decrease repulsive forces, based on merely chemical analysis [50].

Exploring P2 zone (Fig. 2) structural variations show up two kinds of HEA ligands: lactam (2VIZ, 2WF0, 2VJ9, 2VJ7, 2VIE, 2WEZ and 2VJ6 ligands) and sultam derivatives (2VIY, 2WF2, 2WF3, 2WF4, 2VNM and 2WF1 ligands). The first ones are ligands with a B, C, F or G fragment while sultams are ligands with an A, D, E, H or I fragments at P2–P3 zones (Table 1). The biological inhibition trials yield up that sultams appeared more potent than lactams acting as BACE-1 inhibitors but no evidence supporting chemically those differences were presented. This phenomenon stands out attention since previous report indicates that sulfonamides are in general less powerful hydrogen bond acceptors than amides [9]. Our methodology gives a deep insight to this problem, revealing that ASN294 and ARG296 residues IE values at S2 pocket offer a quantitative explanation to these differences; when sultams and lactams are compared, it could be noticed that there is a favoring of ASN294 IE while for ARG296 it is shown a notable decrease in repulsions. IE value differences are in range of 1.5–8.5 and 7–16 kcal/mol for favoring ASN294 and ARG296 residues decreasing repulsion, respectively. The two oxygen atoms in sultam derivatives configure a higher electronic density at P2 zone than lactamic ones which have only a single oxygen atom. As consequence, sultam derivate ligands can offer more electronic density to positive charged ARG296 residue, that act as an electrophile, while increase its acceptor hydrogen bond capacity to interact better with ASN294 residue. These comparative results differentiating both groups are depicted graphically on Fig. 5.

The substitutions made on P3 ligand zone directly affect interactions with THR293 residue, one of the most relevant non-aspartylic polar interactions. The best IE values came from a hydrogen bond between the ligand and hydroxyl group from threonine residue, where the electronegative atoms in the ligand and THR293 residue can act as hydrogen bond donor and/or acceptor atoms. Most of the first generation of HEA transition-state mimetic BACE-1 inhibitors in the study set (2VIE, 2VJ6, 2VJ7, 2VJ9 and 2VNM ligands) has a $–NHC_2H_5$ moiety (C and D fragments, Table 1) acting as a secondary amine and therefore as good hydrogen bond donor atom. In addition, a favored IE value is reported by 2VIZ ligand too. In this case the inhibitor exhibit a $–OC_3H_8$ moiety at P4 zone (B fragment, Table 1) and the oxygen atom acts as a hydrogen bond acceptor while the threonine residue orientate its hydroxyl group to give the hydrogen bond formation, acting as a hydrogen bond donor atom. Meanwhile, heterocycle formation in most of second generation BACE-1 inhibitors (2VNN, 2WEZ, 2WF0, 2WF1, 2WF2 and 2WF4 ligands), where P3–P4 ligand zones (Fig. 2) are involved, leads to a depletion in THR293 interaction. On this case, the nitrogen-cyclic moiety is a tertiary amine and its lone pair is now part of the electron delocalization present in the rings. The aromatic stability in the heterocyclic conjugated

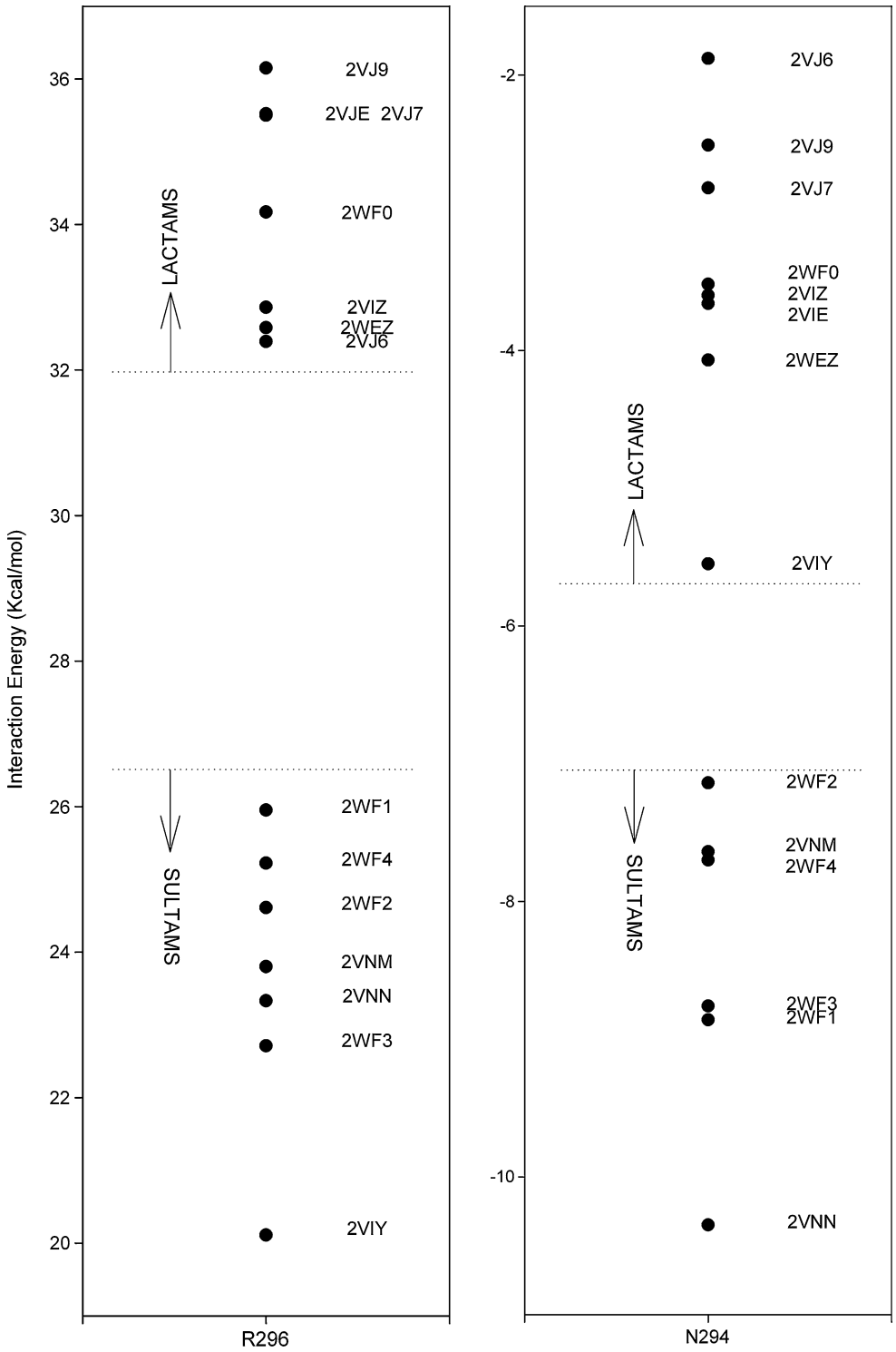

Fig. 5 Differentiation of sultam and lactam type ligands on the basis of the interaction energies with R296 and N294 residues

systems lowers the nitrogen capacity as acceptor hydrogen bond. On the other hand, the unfavorable IE values report by 2VNN and 2WF1 ligands, that share the E fragment, indicate that nitrogen atom position at heterocyclic directly affects THR293 interaction energy magnitude.

The moderately polar TYR132 and TYR259 residues, located on the border between S1 and S1′ areas, and at the top of S2′ zone, respectively, exhibit favorable IE values by virtue of the phenol functionality. TYR132 interacts at P1 and P1′ zones with phenyl and amine groups of the ligand, respectively. Both, non-polar and polar, interactions are considered to be attractive. Beside, variations in TYR259 IE values are explained taking in account P2′ ligand structural modifications: complete non-polar fragments K

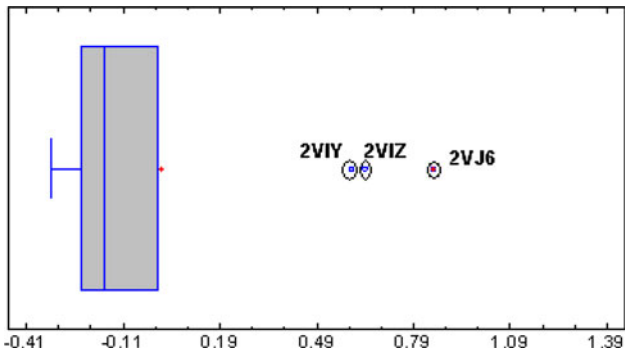

Fig. 6 Boxplot for VAL130 residue IE values

(2VJ9) and L (2VIE) present remarkable IE values as they are in direct contact with TYR259 phenyl group. Another fragments at P2′ zone of the ligand like J (2VIZ, 2VJ6) and the 4-(tetrahydro-2H-pyran) moiety in the 2WF4 ligand, which bear an electronegative oxygen atom, induce a change in the TYR259 hydroxyl group orientation in order to get better the dipole–dipole interactions.

The 2WF4 ligand, which is the only one in the set without a hydroxyethylamine transition state mimetic and displaying a double hydroxyl group at P1′ zone, can achieve excellent IE values, over the rest of ligands, with some residues such as GLN134, THR133, TYR259, ASP93, GLY291 and GLY72, showing that this structural modification could be considered as an good alternative in BACE-1 inhibitor design.

Pearson's coefficient of variation (CV) values are a rough measure of relative dispersion of the interaction energy values for each residue of the BACE-1 active site in our Hydroxyethylamine type inhibitors study group (Table 5). CV values close to zero represent those residues that interact with common areas in all inhibitors, such as the pair of aspartates, PHE169, GLY72, GLY95, GLN134 and TYR132, which interact with hydroxyethylamine core. Oppositely, zero outliers are those interactions whose dispersion is severely affected by the ligand structural modifications, e.g. the pair of serines, VAL130, TYR259, GLY74 and ILE171, residues which are around P2, P′2 and

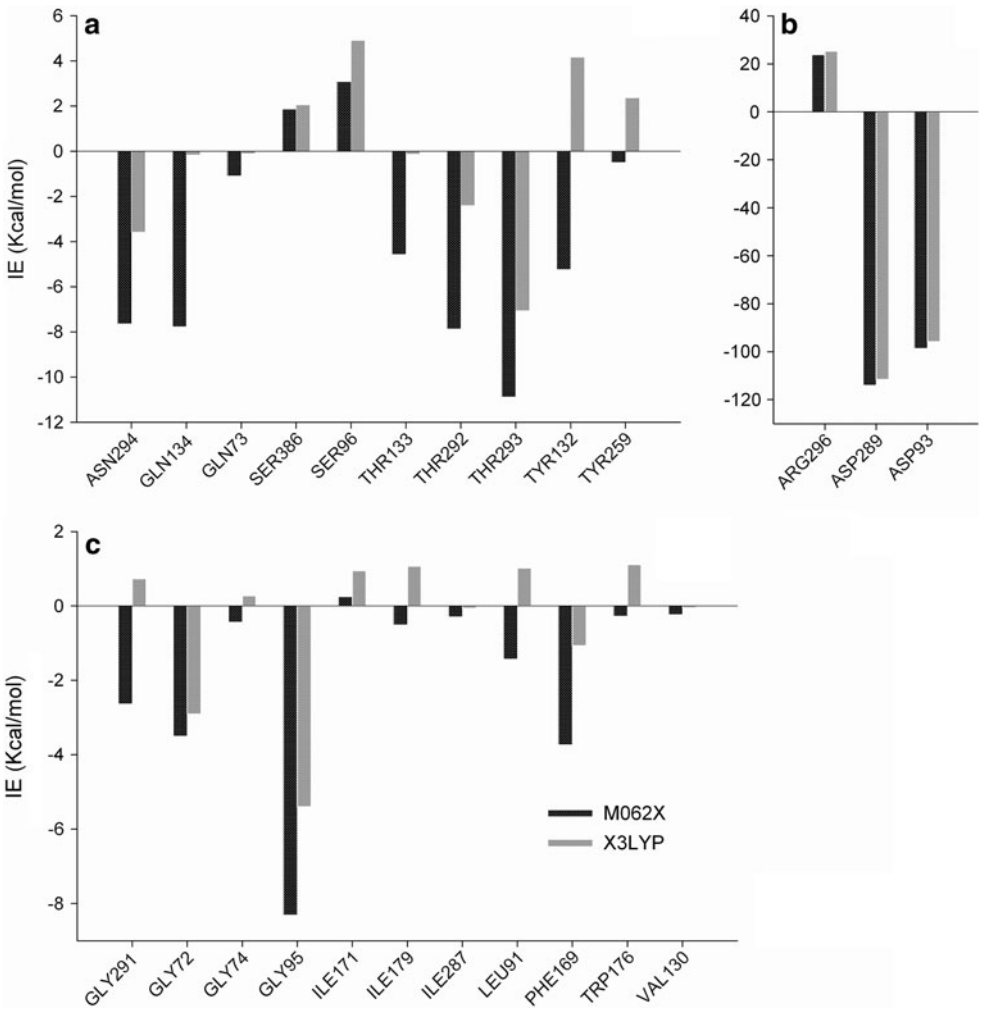

Fig. 7 Graphical comparison between M062X and X3LYP DFT functionals. 2VNM was taken as reference. **a** Polar residues, **b** charged residues and **c** non polar residues

Table 6 Comparison of M062X y X3LYP IE results for selected residues using MP2 as standard reference method

	MP2	M062X	X3LYP
GLN134	−6.82	−7.76	−0.16
GLY291	−1.42	−2.63	0.73
GLY74	−0.43	−0.43	0.27
ILE179	−0.68	−0.51	1.07
LEU91	−1.14	−1.43	1.02
THR133	−4.36	−4.56	−0.12
TRP176	−0.81	−0.27	1.11
TYR132	−5.75	−5.23	4.16
TYR259	−0.75	−0.49	2.36

Interaction energies are expressed in kcal/mol units

P3 areas. The highest CV value is reported for VAL130 (4,171.00%), which is depicted in boxplot (Fig. 6): All hydroxyethylamine inhibitors display negative values of IE except 2VIY, 2VIZ and 2VJ6 ligands, that share the 2-(*N*-cyclohexylpropanamide) moiety (Fragment J, Table 1) which exhibit a repulsion, probably due to proximity of interacting groups or polar-apolar repulsion.

In Tables 2 and 3 are reported the IE values obtained from a level of calculation M062X and X3LYP, and 6-311G(d,p) for DFT functional and basis set, respectively. Additionally, Fig. 7 displays the difference between both DFT functionals taking 2VNM as reference. MP2 method [49] was used as standard for comparison in those cases where couples do not follow the same pattern (Table 6). The results show that both calculation methods are useful for comparative purposes when it is just considered the ion pair interactions (ASP93, ASP289 and ARG296). Further, polar interactions between the small size residues (SER386, SER96, THR293, GLY7 and GLY74) that interact thought hydrogen bond yield also the same type of trend. Nevertheless, for more complete studies, which include hydrophobic interactions, it is recommend the use of M062X functional as it was parameterized to cover the London dispersion forces [25] and it is able to make a description of aromatic stacking interactions that are in good agreement with MP2 theory level [50].

The Table 7 gives the magnitude of the counterpoise corrections for the interaction energies for all residues and ligands. It can be seen from this data that correcting for basis set superposition error is crucial in these calculations,

Table 7 Magnitude of the counterpoise correction, for the electronic interaction energies between amino acid residues at the BACE-1 active site and HEA ligands for M062X and X3LYP DFT functional calculations, in kcal/mol units

	2VIE	2VIZ	2VJ6	2VJ7	2VJ9	2WEZ	2WF0	2VIY	2VNM	2VNN	2WF1	2WF2	2WF3	2WF4
M062X														
ARG296	0.60	0.79	0.70	0.62	0.64	0.54	0.40	0.53	0.93	0.85	0.69	0.99	0.96	0.88
ASN294	2.56	2.54	2.48	2.33	2.37	2.26	2.26	1.76	2.09	2.28	2.51	2.17	2.25	2.08
ASP289	5.36	5.38	5.35	4.52	5.50	4.70	4.47	5.21	4.63	4.48	4.75	4.40	4.44	6.30
ASP93	4.44	4.86	5.07	4.87	4.93	5.30	5.11	4.72	4.87	5.32	4.67	4.81	4.63	5.88
GLN134	3.80	4.43	4.20	4.30	4.05	4.33	4.18	4.09	4.35	4.44	4.23	4.42	4.28	4.11
GLN73	0.37	0.66	0.44	0.41	0.63	0.55	0.45	0.08	0.32	0.30	0.42	0.47	0.29	0.34
GLY291	2.46	2.81	2.56	2.46	2.47	2.63	2.42	2.02	2.53	2.46	2.36	2.69	2.34	3.03
GLY72	0.96	0.56	1.03	0.84	0.91	1.33	0.99	0.01	0.94	1.15	1.11	1.04	1.18	1.22
GLY74	0.96	0.75	0.84	0.83	0.71	0.88	0.54	0.12	0.85	0.79	0.83	0.66	0.50	0.49
GLY95	2.45	2.37	2.44	2.26	1.88	2.31	2.22	2.48	2.27	2.27	2.33	2.19	2.28	1.87
ILE171	0.25	0.22	0.25	0.16	0.27	0.16	0.24	0.09	0.10	0.08	0.10	0.24	0.21	0.14
ILE179	0.14	0.39	0.32	0.23	0.32	0.35	0.25	0.13	0.33	0.24	0.28	0.25	0.19	0.18
ILE287	0.15	0.22	0.19	0.08	0.07	0.04	0.10	0.01	0.19	0.02	0.04	0.02	−0.02	0.47
LEU91	0.38	0.26	0.23	0.32	0.14	0.26	0.21	0.19	0.24	0.13	0.26	0.32	0.22	0.29
PHE169	0.96	1.05	1.04	0.77	1.10	1.14	1.05	0.95	1.03	0.88	0.91	1.01	0.84	0.93
SER386	0.92	0.85	0.85	0.91	0.79	0.74	0.78	0.65	0.81	0.62	0.66	0.79	0.65	0.53
SER96	0.88	1.08	1.11	1.98	1.19	1.41	2.19	1.25	2.07	2.37	1.61	1.35	1.21	0.97
THR133	3.32	2.84	2.87	2.96	3.18	3.27	2.71	3.03	2.92	2.82	2.83	3.20	3.14	3.16
THR292	3.63	3.80	3.45	3.27	3.44	3.51	3.34	2.89	3.31	3.02	3.39	3.06	3.29	3.56
THR293	3.30	3.72	3.45	3.63	3.37	3.37	3.69	1.78	2.62	2.91	2.91	2.18	2.40	2.65
TRP176	0.41	0.44	0.44	0.39	0.23	0.50	0.39	0.30	0.40	0.48	0.26	0.33	0.35	0.16
TYR132	2.17	2.38	2.47	2.98	2.00	2.49	2.84	2.45	2.95	2.92	2.13	2.39	2.38	1.81
TYR259	0.75	1.28	1.22	1.14	0.73	0.79	0.78	1.73	1.03	1.02	0.73	0.65	0.77	0.77

Table 7 continued

	2VIE	2VIZ	2VJ6	2VJ7	2VJ9	2WEZ	2WF0	2VIY	2VNM	2VNN	2WF1	2WF2	2WF3	2WF4
VAL130	0.22	0.19	0.24	0.64	0.06	0.15	0.48	0.05	0.61	0.65	0.00	0.04	0.12	0.02
X3LYP														
ARG296	0.44	0.53	0.36	0.25	0.55	0.71	0.72	0.48	1.47	0.96	0.83	1.07	0.93	0.76
ASN294	2.98	3.02	2.84	2.76	2.97	2.72	2.81	1.90	2.49	2.65	2.98	2.54	2.48	2.44
ASP289	6.60	6.34	6.33	5.15	6.67	5.82	5.15	6.44	5.84	5.57	5.85	5.38	5.22	7.66
ASP93	5.41	5.82	6.16	6.14	6.13	6.53	6.58	5.75	6.26	6.62	5.89	5.84	5.39	7.25
GLN134	4.51	5.17	4.69	4.91	4.79	5.17	5.13	5.15	5.62	5.39	5.09	5.27	5.13	4.73
GLN73	0.56	0.51	0.36	0.41	0.81	0.61	0.58	0.08	0.47	0.29	0.67	0.28	0.47	0.43
GLY291	2.99	3.30	3.02	2.74	3.10	3.37	3.25	2.36	3.16	3.09	3.06	3.12	2.72	3.59
GLY72	1.12	0.65	1.16	1.02	1.44	1.58	1.40	0.20	1.46	1.58	1.71	1.61	1.36	1.82
GLY74	0.99	0.58	0.84	0.93	0.90	1.13	0.76	0.22	1.26	0.97	0.93	1.00	0.43	0.40
GLY95	2.90	2.82	2.98	2.71	2.44	2.82	3.02	2.75	2.87	2.87	3.07	2.80	2.68	2.30
ILE171	0.36	0.06	0.11	0.14	0.32	0.30	0.19	0.05	0.43	0.13	0.17	0.32	0.34	0.08
ILE179	0.25	0.21	0.15	0.03	0.35	0.47	0.46	0.23	0.53	0.27	0.23	0.30	0.08	0.24
ILE287	0.20	0.01	0.20	0.12	0.09	0.16	0.24	0.03	0.42	0.13	0.06	0.20	0.01	0.40
LEU91	0.34	0.06	0.15	0.24	0.25	0.40	0.45	0.14	0.41	0.24	0.48	0.59	0.26	0.19
PHE169	1.11	1.08	0.99	0.86	1.02	1.47	1.46	1.24	1.45	1.11	1.14	1.30	0.97	0.81
SER386	1.13	0.88	1.01	0.81	0.97	1.07	0.90	0.79	1.09	0.65	0.71	0.78	0.82	0.64
SER96	1.03	1.22	1.16	2.12	1.44	1.62	2.59	1.34	2.77	3.04	1.93	1.61	1.43	1.19
THR133	3.95	3.48	3.44	3.55	3.91	4.15	3.70	3.65	3.61	3.65	3.88	4.15	3.95	3.96
THR292	4.21	4.38	3.92	3.75	3.98	4.23	4.02	3.18	4.03	3.60	4.03	3.67	3.74	4.16
THR293	3.94	4.34	4.02	4.36	4.27	4.16	4.41	2.02	3.54	3.50	3.55	2.78	2.94	2.92
TRP176	0.37	0.41	0.44	0.29	0.52	0.56	0.58	0.53	0.62	0.59	0.55	0.57	0.24	0.30
TYR132	2.45	2.70	2.74	3.35	2.27	2.78	3.46	2.56	3.65	3.58	2.45	2.43	2.61	2.12
TYR259	0.73	1.45	1.36	1.02	0.94	1.07	0.78	1.88	1.43	1.27	0.87	0.59	0.75	0.98
VAL130	0.06	0.01	0.04	0.76	0.00	0.20	0.65	0.12	0.95	0.77	0.04	0.05	0.07	0.21

especially for those ones where the residues are very close to the ligand (GLY95, TYR132,Q134, PHE169, TYR259 and GLY291) or have a strong IE with them (ASP93, THR133, ASP289, THR292, THR293 and ASN294). Weak interactions like most of the hydrophobic ones (LEU91, VAL130, ILE171 and I287) exhibit negligible BSSE corrections, since the residues-ligand distances are large.

Conclusions

Ligand-residue counterpoise corrected electronic interaction energies provide interesting insight into the importance of ligand structural variations for binding in the active site of BACE-1 enzyme, and in proteins in general. Additionally, it offers a general and particular quantitative description to explore in detail the enzyme active site-ligand interactions. The M062X and X3LYP approach for quantum chemistry calculations show the importance of polar interactions as these are predominant in this system, being indispensable those ones with aspartate charged residues as contributes with over 90% of the total attractive interactions. In contrast, the design of compounds with a decrease in ARG296 repulsion interactions would lead to better BACE-1 inhibitors. Correcting for basis set superposition errors looks to be crucial for most of strong interaction energy calculation and failure to perform basis set superposition error corrections would result in unpredictable errors.

Interaction energies reported in this work are in agreement with chemical findings described to be important for the activity of this family of BACE-1 inhibitors and constitute a solid background to be considered for the future design of hydroxyethylamine type inhibitors.

Acknowledgments We want to express our gratitude to professor Abdul-Rahman Allouche for his very kind cooperation, attending our requirements for Gabedit source modification necessary for the calculations. We also acknowledge COLCIENCIAS and the Universidad of Cartagena for supporting and funding our research group. The authors greatly appreciate feedback and suggestions made by anonymous referees.

References

1. Vassar R (2002) Adv Drug Deliv Rev 54:1589–1602
2. Evin G, Weidemann A (2002) Neurobiol Aging 22:799–809
3. McGeer PL, McGeer EG (2001) Neurobiol Aging 22:799–809
4. Ghosh AK, Gemma S, Tang J (2008) Neurotherapeutics 5:399–408
5. Rodriguez-Barrios F, Gago F (2004) Curr Top Med Chem 4:991–1007
6. Clarke B, Demont E, Dingwall C, Dunsdon R, Faller A, Hawkins J, Hussain I, MacPherson D, Maile G, Matico R, Milner P, Mosley J, Naylor A, O'Brien A, Redshaw S, Riddell D, Rowland P, Soleil V, Smith KJ, Stanway S, Stemp G, Sweitzer S, Theobald P, Vesey D, Walter DS, Ward J, Wayne G (2008) Bioorg Med Chem Lett 18:1011–1016
7. Clarke B, Demont E, Dingwall C, Dunsdon R, Faller A, Hawkins J, Hussain I, MacPherson D, Maile G, Matico R, Milner P, Mosley J, Naylor A, O'Brien A, Redshaw S, Riddell D, Rowland P, Soleil V, Smith KJ, Stanway S, Stemp G, Sweitzer S, Theobald P, Vesey D, Walter DS, Ward J, Wayne G (2008) Bioorg Med Chem Lett 18:1017–1021
8. Beswick P, Charrier N, Clarke B, Demont E, Dingwall C, Dunsdon R, Faller A, Gleave R, Hawkins J, Hussain I, Johnson CN, MacPherson D, Maile G, Matico R, Milner P, Mosley J, Naylor A, O'Brien A, Redshaw S, Riddell D, Rowland P, Skidmore J, Soleil V, Smith KJ, Stanway S, Stemp G, Stuart A, Sweitzer S, Theobald P, Vesey D, Walter DS, Ward J, Wayne G (2008) Bioorg Med Chem Lett 18:1022–1026
9. Charrier N, Clarke B, Cutler L, Demont E, Dingwall C, Dunsdon R, Hawkins J, Howes C, Hubbard J, Hussain I, Maile G, Matico R, Mosley J, Naylor A, O'Brien A, Redshaw S, Rowland P, Soleil V, Smith KJ, Sweitzer S, Theobald P, Vesey D, Walter DS, Wayne G (2009) Bioorg Med Chem Lett 19:3664–3668
10. Charrier N, Clarke B, Demont E, Dingwall C, Dunsdon R, Hawkins J, Hubbard J, Hussain I, Maile G, Matico R, Mosley J, Naylor A, O'Brien A, Redshaw S, Rowland P, Soleil V, Smith KJ, Sweitzer S, Theobald P, Vesey D, Walter DS, Wayne G (2009) Bioorg Med Chem Lett 19:3669–3673
11. Charrier N, Clarke B, Cutler L, Demont E, Dingwall C, Dunsdon R, Hawkins J, Howes C, Hubbard J, Hussain I, Maile G, Matico R, Mosley J, Naylor A, O'Brien A, Redshaw S, Rowland P, Soleil V, Smith KJ, Sweitzer S, Theobald P, Vesey D, Walter DS, Wayne G (2009) Bioorg Med Chem Lett 19:3674–3678
12. Truong AP, Probst GD, Aquino J, Fang L, Brogley L, Sealy JM, Hom RK, Tucker JA, Jhn V, Tung JS, Pleiss MA, Konradi AW, Sham HL, Dappen MS, Tóth G, Yao N, Brecht E, Pan H, Artis DR, Ruslim L, Bova MP, Sinha S, Yednock TA, Zmolek W, Quinn KP, Sauer JM (2010) Bioorg Med Chem Lett 20:4789–4794
13. Gao J, Winslow SL, Vander Velde D, Aubé J, Borchardt RT (2001) J Pept Res 57:361–373
14. Hussain I, Hawkins J, Harrison D, Hille C, Wayne G, Cutler L, Buck T, Walter D, Demont E, Howes C, Naylor A, Jeffrey P, Gonzalez MI, Dingwall C, Michel A, Redshaw S, Davis JB (2007) J Neurochem 100:802–809
15. Salum LB, Valadares NF (2010) J Comput Aided Mol Des 24:803–817
16. Rizzi L, Vaiana N, Sagui F, Genesio E, Pilli E, Porcari V, Romeo S (2009) Protein Pept Lett 16:86–90
17. Manoharan P, Vijayan RSK, Ghoshal NJ (2010) Comput Aided Mol Des 24:843–864
18. Pandey A, Mungalpara J, Mohan CG (2010) Mol Divers 14:39–49
19. Utkov H, Livengood M, Cafiero M (2010) Annu Rep Comput Chem 10:96–112
20. Söderhjelm P, Kongsted J, Ryde U (2010) J Chem Theor Comput 6:1726–1737
21. Söderhjelm P, Aquilante F, Ryde U (2009) J Phys Chem B 113:11085–11094
22. Alzate-Morales JH, Contreras R, Soriano A, Tuñon I, Silla E (2007) Biophys J 92:430–439
23. Zhao Y, Truhlar D (2008) Theor Chem Acc 120:215–241
24. Xu X, Goddard WA (2004) PNAS 101:2673–2677
25. Valdes H, Pluháckova K, Pitonák M, Rezác J, Hobza P (2007) Phys Chem Chem Phys 10:2747–27578
26. Cole SL, Vassar R (2007) Molecular Neurodegener 2:22
27. Bernstein FC, Koetzle TF, Williams GJ, Meyer EF, Brice MD, Rodgers JR, Kennard O, Shimanouchi T, Tasumi M (1977) Eur J Biochem 80:319–324
28. Accelrys Software Inc. (2010) DSV 3.0
29. Ren P, Ponder JW (2003) The J Phys Chem B 107:5933–5947
30. Chesmitry Stewart Computational (2009) MOPAC 2009 Version 10040L
31. Klamt A, Schüümann GJ (1993) J Chem Soc Perkin Trans 25:799–805
32. Stewart JJ (2009) Mol Model 15:765–805
33. Stewart JJ (2007) Mol Model 13:1173–1213
34. Yamazaki T, Nicholson LK, Wingfield P, Stahl SJ, Kaufman JD, Eyermann CJ, Hodge CN, Lam PYS, Torchia DA (1994) J Am Chem Soc 116:10791–10792
35. Hyland LJ, Tomaszek TA, Roberts GD, Carr SA, Magaard VW, Bryan HL, Fakhoury SA, Moore ML, Minnich MD, Culp JS (1991) Biochemistry 30:8441–8453
36. Hyland LJ, Tomaszek TA, Meek TD (1991) Biochemistry 30:8454–8463
37. Yu N, Hayik SA, Wang B, Liao N, Reynolds CH, Merz KM (2006) J Chem Theor Comput 2:1057–1069
38. Polgar T, Keserü GM (2005) J Med Chem 48:3749–3755
39. Rajamani R, Reynolds CH (2004) J Med Chem 47:5159–5166
40. Park H, Lee S (2003) J Am Chem Soc 125:16416–16422
41. Huang D, Caflisch A (2004) J Med Chem 47:5791–5797
42. Diez y Riega H, Rincón L, Almeida R (2003) J Phys Org Chem 16:107–113
43. Frisch MJ, Trucks GW, Schlegel HB, Scuseria GE, Robb MA, Cheeseman JR, Scalmani G, Barone V, Mennucci B, Petersson GA, Nakatsuji H, Caricato M, Li X, Hratchian HP, Izmaylov AF, Bloino J, Zheng G, Sonnenberg JL, Hada M, Ehara M, Toyota K, Fukuda R, Hasegawa J, Ishida M, Nakajima T, Honda Y, Kitao O, Nakai H, Vreven T, Montgomery JA, Peralta JE, Ogliaro F, Bearpark M, Heyd JJ, Brothers E, Kudin KN, Staroverov VN, Kobayashi R, Normand J, Raghavachari K, Rendell A, Burant JC, Iyengar SS, Tomasi J, Cossi M, Rega N, Millam NJ, Klene M, Knox JE, Cross JB, Bakken V, Adamo C, Jaramillo J, Gomperts R, Stratmann RE, Yazyev O, Austin AJ, Cammi R, Pomelli C, Ochterski JW, Martin RL, Morokuma K, Zakrzewski VG, Voth GA, Salvador P, Dannenberg JJ, Dapprich S, Daniels AD, Farkas Ö, Foresman JB, Ortiz JV, Cioslowski J, Fox DJ (2009) Gaussian, Inc., Wallingford
44. Allouche AR (2011) J Comput Chem 32:174–182
45. Boys SF, Bernardi F (1970) Mol Phys 19:553–566
46. Almlof J, Helgaker T, Taylor PR (1988) J Phys Chem 92:3029–3033
47. Stigler SM (2008) Stat Sci 23:261–271
48. Clarke B, Cutler L, Demont E, Dingwall C, Dunsdon R, Hawkins J, Howes C, Hussain I, Maile G, Matico R, Mosley J, Naylor A, O'Brien A, Redshaw S, Rowland P, Soleil V, Smith KJ, Sweitzer S, Theobald P, Vesey D, Walter DS, Wayne G (2010) Bioorg Med Chem Lett 20:4639–4644
49. Head-Gordon M, Pople JA, Frisch MJ (1988) Chem Phys Lett 153:503–506
50. Gu J, Wang J, Leszczynski J, Xie Y, Schaefer HF III (2008) Chem Phys Lett 459:164–166